






Muscle contractile properties directly influence shared synaptic inputs to spinal motor neurons

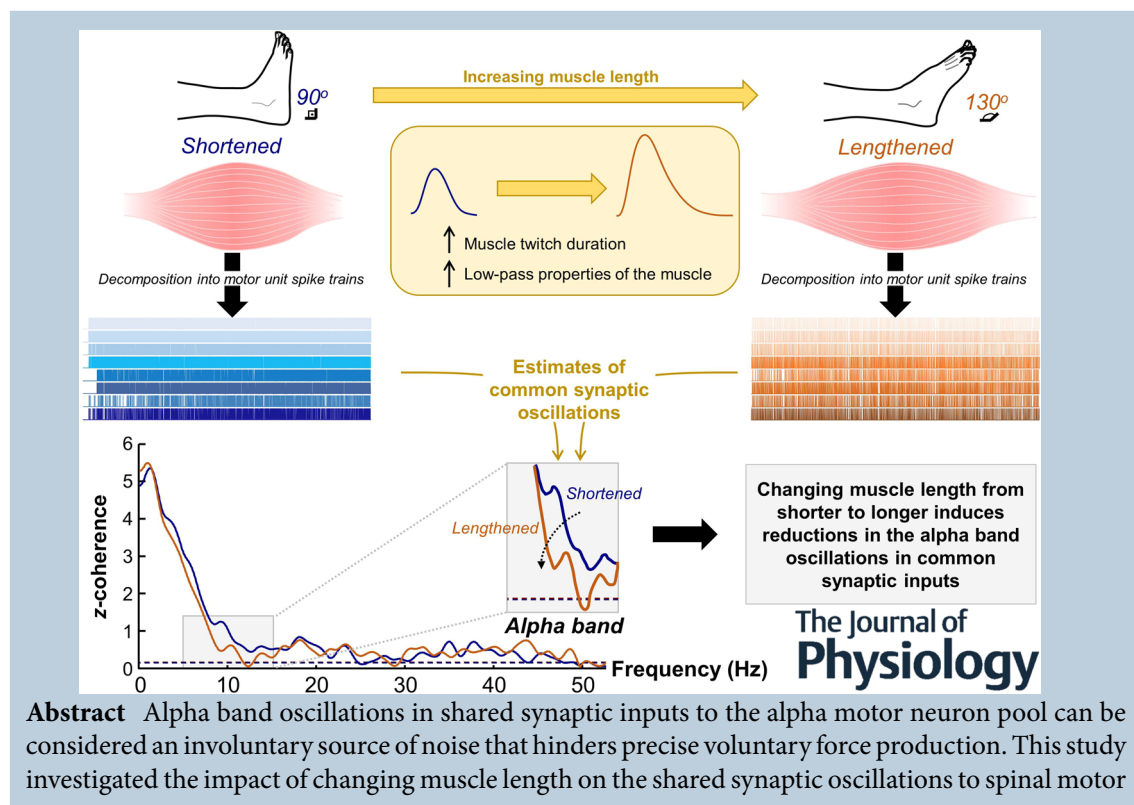
Hélio V. Cabral¹ , J. Greig Inglis¹ , Alessandro Cudicio¹ , Marta Cogliati¹ , Claudio Orizio¹, Utku S. Yavuz² and Francesco Negro¹ 

¹Department of Clinical and Experimental Sciences, Università degli Studi di Brescia, Brescia, Italy

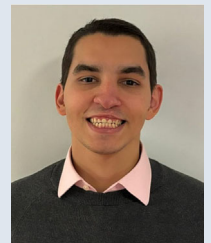
²Biomedical Signals and Systems, University of Twente, Enschede, Netherlands

Handling Editors: David Wyllie & James Coxon

The peer review history is available in the Supporting Information section of this article (<https://doi.org/10.1113/JP286078#support-information-section>).



Hélio Cabral is currently employed as a Postdoctoral Research Fellow in the Department of Clinical and Experimental Sciences at the Università degli Studi di Brescia, Italy. In March 2020, he completed his PhD in Biomedical Engineering at the Universidade Federal do Rio de Janeiro, Brazil. Subsequently, he worked for 2 years as a Postdoctoral Research Fellow at the University of Birmingham, UK. His research combines electrophysiological and biomechanical measures with signal processing methods to investigate the neural control of movement in a broad range of topics, including motor control, neural plasticity, exercise and neuromuscular disorders.



This article was first published as a preprint. Cabral HV, Inglis JG, Cudicio A, Cogliati M, Orizio C, Yavuz U, Negro F. 2023. Muscle contractile properties directly influence shared synaptic inputs to spinal motor neurons. bioRxiv. <https://doi.org/10.1101/2023.11.30.569389>

neurons, particularly in the physiological tremor band. Fourteen healthy individuals performed low-level dorsiflexion contractions at ankle joint angles of 90° and 130°, while high-density surface electromyography (HDsEMG) was recorded from the tibialis anterior (TA). We decomposed the HDsEMG into motor units spike trains and calculated the motor units' coherence within the delta (1–5 Hz), alpha (5–15 Hz), and beta (15–35 Hz) bands. Additionally, force steadiness and force spectral power within the tremor band were quantified. Results showed no significant differences in force steadiness between 90° and 130°. In contrast, alpha band oscillations in both synaptic inputs and force output decreased as the length of the TA was moved from shorter (90°) to longer (130°), with no changes in delta and beta bands. In a second set of experiments (10 participants), evoked twitches were recorded with the ankle joint at 90° and 130°, revealing longer twitch durations in the longer TA muscle length condition compared to the shorter. These experimental results, supported by a simple computational simulation, suggest that increasing muscle length enhances the muscle's low-pass filtering properties, influencing the oscillations generated by the Ia afferent feedback loop. Therefore, this study provides valuable insights into the interplay between muscle biomechanics and neural oscillations.

(Received 1 December 2023; accepted after revision 18 April 2024; first published online 6 May 2024)

Corresponding author: F. Negro: Department of Clinical and Experimental Sciences, Università degli Studi di Brescia, Viale Europa 11, Brescia 25121, Italy. Email: francesco.negro@unibs.it

Abstract figure legend Motor unit spike trains were decomposed from high-density surface electromyograms recorded from the tibialis anterior (TA) muscle at two different ankle joint angles: 90° (shortened) and 130° (lengthened). To assess changes in shared synaptic input to motor neurons between muscle lengths, we quantified the average z-coherence of motor unit spike trains within the delta, alpha, and beta bands. Changing the TA muscle length from shorter to longer decreased alpha band oscillations in both shared synaptic inputs and force power, with no significant changes in delta and beta bands. Additionally, longer TA twitch durations were observed when the muscle was lengthened compared to shortened, indicating alterations in the low-pass filtering characteristics of the muscle. These experimental results, supported by computational simulations, suggest that the increased motor unit twitch duration resulting from increased muscle length directly influences the amplitude of the alpha band oscillations through a proprioceptive (Ia) afferent loop.

Key points

- We investigated whether changes in muscle length, achieved by changing joint position, could influence common synaptic oscillations to spinal motor neurons, particularly in the tremor band (5–15 Hz).
- Our results demonstrate that changing muscle length from shorter to longer induces reductions in the magnitude of alpha band oscillations in common synaptic inputs. Importantly, these reductions were reflected in the oscillations of muscle force output within the alpha band.
- Longer twitch durations were observed in the longer muscle length condition compared to the shorter, suggesting that increasing muscle length enhances the muscle's low-pass filtering properties.
- Changes in the peripheral contractile properties of motor units due to changes in muscle length significantly influence the transmission of shared synaptic inputs into muscle force output.
- These findings prove the interplay between muscle mechanics and neural adaptations.

Introduction

The generation of voluntary movement relies on a sequence of integrated processes that culminate in the production and modulation of a muscle force output (Enoka & Farina, 2021; Heckman & Enoka, 2012). The

pool of alpha motor neurons plays a pivotal role in these complex processes by integrating common and independent synaptic inputs into individual motor unit action potential train outputs, which are subsequently propagated to the active muscle (Duchateau & Enoka, 2011; Ishizuka et al., 1979; Lemon, 2008). Rather than

acting independently, the resultant discharge times of individual motor units exhibit similar behaviours, as evidenced by the high correlation between their activities (Datta & Stephens, 1990; De Luca et al., 1982; Farmer et al., 1993; Hug et al., 2023; Kirkwood & Sears, 1978; Sears & Stagg, 1976). These common fluctuations observed in the output of neuronal ensembles have been attributed to shared synaptic projections across motor neuron pools, which may have cortical or spinal origins (Bremner et al., 1991; Farina et al., 2014; Farmer et al., 1993; Negro & Farina, 2011; Nordstrom et al., 1992). Given the main role of cortical pathways in the voluntary control of movement, shared projections from the motor cortex are believed to be the primary source of correlation between motor neuron spike trains, particularly in the delta (associated with voluntary force corrections) and beta bands (linked with corticomuscular coherence) (Baker et al., 1997; Bräcklein et al., 2022; Conway et al., 1995; Datta & Stephens, 1990; Datta et al., 1991; Kirkwood & Sears, 1978). These shared projections hold an important functional role, as the synergistic activation of multiple motor neurons by these common oscillations facilitates the optimization of the motor control system (Berniker et al., 2009; d'Avella & Bizzi, 2005; Laine et al., 2015).

The shared cortical projections are not the exclusive source of correlations between motor unit spike trains in human muscles. Notably, during isometric voluntary contractions, the force output exerted includes a significant portion of involuntary rhythmic fluctuations in the frequency range of 5–15 Hz (alpha band), often associated with physiological tremor (Lippold, 1971; McAuley & Marsden, 2000). These oscillations, resulting from physiological tremor, can be partially attributed to afferent inputs originating from the active muscles themselves, which project to the motor neuron pool (Christakos et al., 2006; Cresswell & Löscher, 2000; Hagbarth & Young, 1979; Laine et al., 2016; Lippold, 1970). More specifically, the spinal stretch reflex establishes a feedback loop that functions as a servo-mechanism system aimed at maintaining stability at the muscle level (Lippold, 1971). Due to inherent delays in signal transmission within this feedback loop, oscillations at resonant frequencies, which were not present in the initial input of the motor neuron pool, tend to emerge (Halliday & Redfearn, 1956; Lippold, 1970; Lippold, 1971). Consequently, the resonance behaviour can lead to oscillations at these frequencies in the neural drive to the active muscle, resulting in variations in the steadiness of the muscle force output (Inglis & Gabriel, 2021; McAuley & Marsden, 2000). In this context, physiological tremor oscillations can be seen as noise oscillations in the neural drive, transmitted to the force output, that interfere with precise voluntary force production. Previous studies have suggested that increased fluctuations in force output steadiness are likely the result of common noise in the

neural commands sent to active motor units (Feeney et al., 2018; Negro et al., 2009; Thompson et al., 2018). Therefore, understanding the mechanisms involved in the modulation of alpha band oscillations (physiological tremor) is extremely important in the investigation of neuromuscular control.

Recent investigations have demonstrated that oscillations in force output within the alpha band can be modulated by a range of factors. These factors include changes in nociceptive input (Yavuz et al., 2015), enhancement of serotonin availability by pharmacological means (Henderson et al., 2022) and alterations in the demands of a visuomotor task (Laine et al., 2014). Of particular interest are changes in muscle length, which have been shown to exert a direct influence on alpha oscillations in force output, with shorter muscle lengths being associated with an increase in physiological tremor (Jalaleddini et al., 2017). A potential explanation for this phenomenon, derived from computational simulations, is related to alterations in the modulation of the gamma static fusimotor drive following changes in muscle length (Jalaleddini et al., 2017). Additionally, these changes may occur as a result of mechanistic changes at the periphery, such as the amount of musculoskeletal stiffness or joint laxity (Clamann & Schelhorn, 1988; Powers & Binder, 1991; Rack & Westbury, 1969). Furthermore, changing the muscle length affects the average twitch profile of motor units, resulting in changes to the muscle's low-pass filtering properties when converting motor unit spike trains into mechanical movements about a joint (Bawa & Stein, 1976; Mannard & Stein, 1973; Rack & Westbury, 1969). Specifically, longer muscle lengths result in longer twitch durations, subsequently intensifying the low-pass filtering effect of the neural drive to the muscle. The enhanced effect of filtering the averaged motor unit twitch, in turn, may directly influence the behaviour of the afferent loop, leading to modulated oscillations in physiological tremor. However, whether this phenomenon occurs remains unexplored in the literature, and, to date, no previous study has experimentally investigated the effect of altered muscle length on alpha oscillations in common synaptic inputs to the alpha motor neuron pool.

In the present study, we aimed to investigate whether changes in muscle length could influence the common synaptic oscillations to spinal motor neurons, particularly in the tremor band (5–15 Hz). To achieve this, we decomposed motor unit spike trains from high-density surface electromyograms recorded from the tibialis anterior (TA) at two different ankle joint angles. Additionally, to interpret the results derived from the motor unit spike trains, we conducted a second set of experiments, combined with computational simulations, to investigate how changes in muscle length affect the low-pass characteristics of the TA's electrically evoked potentials (twitches).

Methods

Ethical approval

All participants provided written informed consent before starting the experiments. This study conformed to the standards set by the latest version of the *Declaration of Helsinki*, except for registration in a database, and was approved by the ethics committee of the University of Brescia (code NP2490).

Participants

Fourteen healthy individuals (1 female; mean \pm SD: 26 \pm 3 years; 180 \pm 7 cm; 79 \pm 9 kg) volunteered to participate in this study. All participants were free of any neuromuscular abnormalities and had no history of lower limb injury or lower leg pain that would impact their ability to produce voluntary contractions.

Experimental protocol

The study consisted of a single experimental session lasting 1 h. Participants were comfortably seated with their dominant leg (all right leg) placed on a custom-built jig designed to isolate the ankle joint during dorsiflexion contractions. The right knee was fully extended, the hip was flexed at 70° (0° being the hip fully extended), and the right foot was fixed with straps to an adjustable footplate that held the ankle at the specified joint angles. The footplate was connected to a load cell (SM-500 N, Interface, Scottsdale, AZ, USA) to record the dorsiflexion isometric force produced by the dorsiflexors, more specifically the TA (Fig. 1A). Additional straps were placed around the thigh and knee to ensure the force produced relied solely on the dorsiflexor muscles. The subjects were asked to keep their left leg straight and relaxed on the side of the jig.

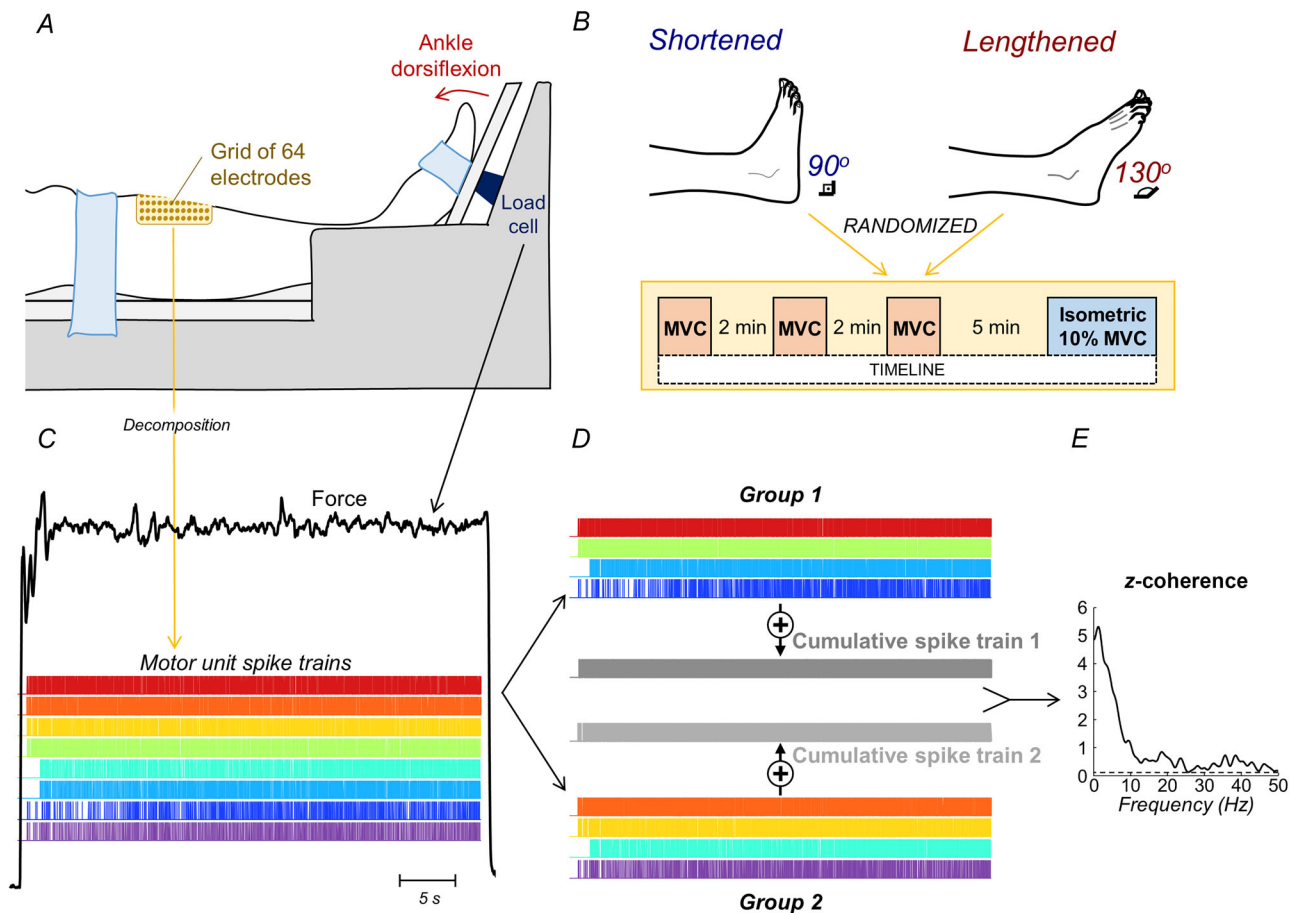


Figure 1. Experimental set-up and motor unit analysis

A, schematic representation of the participants' foot position for measuring dorsiflexion isometric force. High-density surface electromyograms (HDsEMG) were acquired from the tibialis anterior (TA) using a grid of 64 electrodes. B, ankle joint angles were selected to represent conditions where the TA was shortened (90°) and lengthened (130°). The tasks performed for each angle are shown in the yellow box. C–E, steps involved in the motor unit analysis. After decomposition from the HDsEMG recordings (C), the cumulative spike trains of two equally sized groups of motor units were obtained (D), and the coherence between them was calculated (E).

Voluntary contractions. All experimental tasks were repeated for two different ankle joint angles: 90° (0° of plantar flexion) and 130° (40° of plantar flexion). These angles were selected to represent conditions in which the TA muscle was shortened (90°) and lengthened (130°) (top part of Fig. 1B). The condition order was randomized across participants, and a minimum of 10 min of rest was provided between the conditions. For each condition, participants repeated the same experimental protocol (bottom part of Fig. 1B). Each participant performed three voluntary maximum isometric contractions (MVCs) for 3 s, with a 2 min rest between each bout. The greatest value across the three MVCs was considered the maximal isometric dorsiflexion force and used as a reference to set the target of the submaximal force outputs of the corresponding condition. Subsequently, participants underwent a short familiarization period, during which they were instructed to exert isometric ankle dorsiflexion at 10% MVC for approximately 10 s. This familiarization task was repeated (up to a maximum of five times) for both conditions to ensure that participants could maintain the force output as steadily as possible at the target level, which a researcher visually assessed. Following the familiarization period, participants were instructed to perform an isometric dorsiflexion contraction following a trapezoidal profile. For both conditions (90° and 130°), the profile involved a linear increase at a rate of 5% MVC/s, a plateau at 10% MVC for 40 s, and a linear decrease at a rate of 5% MVC/s. The target force output was set at 10% MVC, as the TA is typically activated around this force output during daily activities such as locomotion (Kaneda et al., 2008). Visual feedback from the target and produced dorsiflexion force output were displayed on a computer monitor positioned ~1 m in front of the participant.

Evoked contractions. To assess the effect of muscle length changes on the TA twitch characteristics, we conducted a second set of experiments in 10 healthy individuals (4 females; mean \pm SD: 28 \pm 4 years; 177 \pm 11 cm; 71 \pm 15 kg) (four participants in common with the voluntary contractions). During experiments, electrical stimulation was applied at rest to the common peroneal nerve of the right leg while participants were positioned as described in the first set of experiments. First, a round cathode electrode (20 mm diameter; Spes Medica, Genova, Italy) filled with conductive paste was placed on the skin posterior and inferior to the head of the fibula and a rectangular anode electrode (size 50 \times 100 mm; UltraStim, Axelgaard Manufacturing Co., Fallbrook, CA, USA) was positioned on the opposite side of the knee. The posterior inferior region to the head of the fibula was identified through palpation by an experienced researcher. Once the stimulating electrode was fixed in position, the current intensity leading to the largest evoked dorsiflexion

force output response was defined using a staircase current profile. Specifically, a train of rectangular pulses (200 μ s duration; 1 Hz frequency) with increasing amplitudes (staircase protocol) was delivered until no clear increase in dorsiflexion force output could be visualized; this level was defined as the maximal stimulation intensity. After a 90 s period, rectangular pulses (200 μ s duration; 0.15 Hz frequency) were applied to electrically evoke twitches from the TA for the same ankle joint angles as the voluntary contractions: 90° (0° of plantar flexion) and 130° (40° of plantar flexion). When the ankle joint was placed at an angle of 90° this shortened the TA muscle length, while at 130° the TA muscle length was lengthened. For each condition, 15 supramaximal evoked potentials (20% over the maximal stimulation intensity defined during the staircase protocol) were delivered to the participant. The order of ankle joint angle was randomized with 90 s intervals between each train of stimulation.

Data collection

High-density surface electromyograms (HDsEMG) were acquired from the TA during the submaximal isometric task using a two-dimensional adhesive grid (GR08MM1305; 8 mm inter-electrode distance; OT Bioelettronica, Turin, Italy). The grid consisted of 64 electrodes arranged in 13 rows by 5 columns, with one missing channel in the top left corner. The grid was positioned longitudinally on the TA muscle belly, which was determined via palpation (Fig. 1A). Prior to electrode placement, the area was shaved, mildly abraded (EVERI, Spes Medica) and cleaned. The electrode–skin contact was ensured by filling the foam cavities with conductive paste (AC cream, Spes Medica). The reference electrode was positioned on the right ankle at the level of the malleoli. HDsEMG and force outputs were digitized synchronously at a sampling frequency of 2048 Hz using a 12-bit A/D converter (10–500 Hz bandwidth; EMG-USB2+, OT Bioelettronica). HDsEMG signals were recorded in monopolar derivation and amplified to maximize signal resolution while avoiding saturation.

Data analysis

Force output, HDsEMG, and evoked twitches were analysed offline using MATLAB (version 2022b, The MathWorks, Natick, MA, USA) custom-written scripts.

Force output

The central 30 s of the force outputs acquired during submaximal dorsiflexion contractions were used for all analyses. Initially, force outputs were low-pass filtered at 15 Hz using a third-order Butterworth filter. Sub-

sequently, the power spectral density of force output was estimated using Welch's method (implemented with the *pwelch* function in MATLAB; 1 s Hanning windows with 1948 samples of overlap). For each condition (90° and 130°), the mean power within the alpha band (5–15 Hz) was calculated and retained for further analysis. Additionally, the coefficient of variation (CoV) of force was estimated to quantify the variation of force output at each ankle joint angle. To ensure that the CoV results were not influenced by the chosen window (i.e. central 30 s of force output), the CoV of force considering the 30 s steadiest portion within the 40 s plateau region was also determined. To this end, a 30 s moving window with one sample step was used throughout the 40 s plateau region. Then, the CoV was calculated for each window (totalling 20,481 values), and the minimum value was selected.

HDsEMG decomposition and estimates of common synaptic input

The steps involved in the HDsEMG analysis are schematically represented in Fig. 1C–E. First, monopolar HDsEMG signals were bandpass filtered with a third-order Butterworth filter (20–500 Hz cut-off frequencies). After visual inspection, bad channels, due to contact problems or artifacts, were discarded (mean \pm SD: 2 ± 1 channels for both 90° and 130°). The HDsEMG signals were then decomposed into their constituent motor unit spike trains using a convolutive blind-source separation algorithm (Negro et al., 2016). Briefly, after extending and whitening HDsEMG signals, a fixed-point algorithm that seeks sources that maximize a measure of sparsity was applied to identify the sources (i.e. motor unit spike trains; Fig. 1C). The spikes were separated from the noise using *K*-means and, while iteratively updating the motor unit separation vectors, the discharge time estimation was further refined by minimizing the CoV of the inter-spike intervals. This decomposition method has been extensively applied to assess the activity of single TA motor units (Cogliati et al., 2020; Cudicio et al., 2022; Negro et al., 2016). After the automatic identification of motor units, missed or misidentified motor unit discharges which produced non-physiological discharge rates (<4 pulses per second or >50 pulses per second; Negro et al. 2009) were manually identified and iteratively edited by an experienced operator, and the subsequent motor unit spike trains were re-estimated (Hassan et al., 2020; Martinez-Valdes et al., 2017). This approach has been shown to be highly reliable across operators (Hug et al., 2021).

Similar to the force output analysis, all the motor units decomposed from the experimental data were examined during the 30-s window centred midway through the force output plateau. This section was chosen to exclude peri-

ods of force output transition at the beginning and end of the trapezoidal contraction (McManus et al., 2019). In addition, motor units were discarded from the analysis when they did not discharge continuously for at least 20 s in the selected region. Coherence analysis was used to estimate the level of common synaptic input to the motor neuron pool (Castronovo, Negro et al., 2015; Negro & Farina, 2012; Rossato et al., 2022). Coherence was estimated between cumulative spike trains (CST), each comprising a minimum of two motor unit spike trains. Therefore, only participants with at least four motor units identified in each condition were included in the coherence analysis. First, the identified motor units from each condition were randomly divided into two equally sized groups (Fig. 1D). The number of motor units included in each group was half of the minimal number of motor units identified across conditions. Thus, if 18 and 12 motor units were detected for the 90° and 130° angles respectively, six motor units were included in each group. The discharge times in each group were then summed to obtain two CSTs (Fig. 1D). Coherence was calculated between the two detrended CSTs using Welch's periodogram with a 1 s Hanning window with an overlap of 95% (Fig. 1E). This procedure was repeated for up to 100 randomly chosen combinations of two groups of motor units, and the average of all permutations was calculated (i.e. pooled coherence) (Castronovo, Negro & Farina, 2015; Rossato et al., 2022). Fisher's *z*-transform was then applied to the pooled coherence estimates using an approximation for coherence calculations with overlapping windows (Gallet & Julien, 2011). Only *z*-scores greater than the confidence level were considered for further analysis. The confidence level was defined for each participant as the mean value of *z*-scores between 250 and 500 Hz, as no significant coherence is expected in this frequency range (Rossato et al., 2022). To investigate changes in common synaptic input between different TA muscle lengths, the means of *z*-coherence within delta (1–5 Hz), alpha (5–15 Hz), and beta (15–35 Hz) bands were calculated. For purposes of visualization only (no statistical analysis), the *z*-coherence values were combined across all participants according to Baker et al. (2003).

Motor unit tracking

To increase the robustness of the analysis, motor units were tracked between ankle joint angles (90° and 130°) based on their shape (Cudicio et al., 2022; Martinez-Valdes et al., 2017). Previous research has demonstrated the successful tracking of motor units across the full range of dorsiflexion motion using this template matching technique (Cudicio et al., 2022). Specifically, two-dimensional representations of the motor unit action potentials of the identified motor units at the

90° angle were cross-correlated with those identified at the 130° angle. Only motor units with highly similar motor unit action potential shapes across the electrode grid were considered as belonging to the same motor unit. Given that variations in muscle length may influence motor unit action potential shapes, we reduced the matching threshold to 0.75, and each match was visually checked by an expert operator. For matched motor units, the level of common synaptic input was estimated as described previously. Additionally, the mean discharge rate was calculated for each matched motor unit.

Coherence between neural drive and force output oscillations

To assess changes in the coupling between oscillations in the neural drive and oscillations in the muscle force output, we calculated the coherence between the neural drive to the muscle and the force output (Negro et al., 2009). For this analysis, the neural drive was estimated by summing the binary discharge trains across all identified motor units (i.e. cumulative spike train) (Negro et al., 2009; Thompson et al., 2018). Moreover, coherence was calculated specifically within the frequency bandwidth relevant to force control (i.e. delta and alpha bands). Similar to the motor unit analyses, we calculated the average of z -coherence to evaluate changes between conditions (shortened and lengthened).

Tibialis anterior evoked twitches

Force outputs acquired during electrically evoked contractions were triggered and averaged at the stimulation times to obtain an averaged twitch force for each ankle joint angle (90° and 130°). The following variables were then extracted from the averaged twitch force profiles: time to peak (t_{peak}), measured as the time elapsed from the first detectable increase in force to the peak twitch; and time to half-peak ($t_{50\% \text{peak}}$), determined as the time from the first detectable increase in force to 50% of decay from the peak twitch. Considering the muscle acts as a low-pass filter when converting the motor unit spike trains into mechanical movement about a joint (Bawa & Stein, 1976; Mannard & Stein, 1973), to explore how the low-pass filter characteristics of TA changed during the different muscle lengths, we computed the normalized magnitude of the frequency response of the twitch force output obtained for each ankle joint angle (90° and 130°). The magnitude of the frequency response represents the gain of the system as a function of frequency. We then calculated the cut-off frequency (f_{co}) in which the gain was attenuated by -3 dB.

Simulations

To further investigate how the contractile properties of motor units influence the transmission of alpha band oscillations into force output, we used a well-established model that simulates the sequence of events from the excitation of an ensemble of motor neurons to the generation of isometric force output. This model, initially proposed by Fuglevand et al. (1993), has since been utilized in various studies (Dideriksen & Negro, 2018; Dideriksen et al., 2012; Dideriksen et al., 2022; Gogeochea et al., 2023; Taylor et al., 2002). The motor neuron parameters were selected based on an exponential distribution across the pool of motor neurons (Fuglevand et al., 1993). Similar to the number of motor units in the TA (Feinstein et al., 1955), the number of motor units in the model was set to 450, of which only those with a minimum discharge rate of 8 pulses per second were fully recruited (Taylor et al., 2002). The input to the motor neuron pool was modelled as a linear summation of common synaptic input to all motor neurons (low-pass filtered Gaussian noise < 15 Hz) and an independent noise input specific to each motor neuron (low-pass filtered Gaussian noise < 50 Hz). The model was implemented in MATLAB, and simulations were conducted with a sampling frequency of 1000 Hz.

To assess the effect of motor unit twitch duration in the transmission of common synaptic noise into force output, we created two distinct models, model 1 and model 2. Specifically, we simulated an increase in the twitch contraction times of individual motor units by modifying the longest contraction duration for the motor unit pool from 80 to 140 ms (parameter T_L in equation 14 of Fuglevand et al. (1993)). This alteration resulted in a median increase of ~ 35 ms in the contraction time of motor unit twitches between the two models. The model with greater contraction time values (model 2) was used to simulate the muscle lengthening condition. Each model was repeated 10 times, as has been done in previous simulation studies (Dideriksen & Negro, 2018; Dideriksen et al., 2022). For each time, we computed the average z -coherence of motor units within delta (1–5 Hz), alpha (5–15 Hz), and beta (15–35 Hz) bands, following the same approach used on the experimental data.

Statistical analysis

All statistical analyses were performed in R (version 4.2.2, R Foundation for Statistical Computing, Vienna, Austria), using the RStudio environment. Considering the non-normality of the data (Kolmogorov–Smirnov test; $P < 0.001$ for all), Wilcoxon's signed-rank test was used to compare the peak MVC, force output steadiness (i.e. CoV of the force output) and mean force output power between conditions. Wilcoxon's signed-rank test was also used to

compare the variables calculated from the TA twitch force outputs (t_{peak} , $t_{50\% \text{peak}}$ and f_{co} of magnitude response) and the motor unit twitch contraction times between the two simulated models.

Linear mixed-effect models (LMM) were applied for all statistical analyses of motor unit data (both matched and unmatched), as they account for the non-independence of data points within each participant. For both experimental and simulated data, the z -coherence averages were compared, separately for delta, alpha and beta bands, using random intercept models with ankle joint angle (90° and 130°) as the fixed effect and participant as the random effect (i.e. z -coherence average = 1 + condition + (1 | participant)). The same statistical model was used to compare the mean discharge rate of matched motor units and the z -coherence values between neural drive and force output oscillations. LMMs were implemented using the package *lmerTest* (Kuznetsova et al., 2017) with the Kenward–Roger method to approximate the degrees of freedom and estimate the P -values. The *emmeans* package was used, when necessary, for multiple comparisons

and to determine estimated marginal means with 95% confidence intervals (Lenth et al., 2019). The values in the text for motor unit results are reported as mean [95% confidence intervals]. All the other values are reported as median (interquartile range) both in the text and in the figures.

All individual data of motor unit discharge times recorded at 90° and 130° are available at <https://doi.org/10.6084/m9.figshare.24631191>.

Results

Dorsiflexion force output

To assess how changes in TA muscle length affected isometric dorsiflexion force production, we compared the peak MVC and force output steadiness between ankle joint angles (90° and 130°). Peak MVC values significantly decreased from 33.1 (28.9–35.9) Nm at 90° to 30.2 (25.6–33.2) Nm at 130° ankle joint angle (Wilcoxon's signed-rank test; $V = 86$; $P = 0.035$). Figure 2A shows

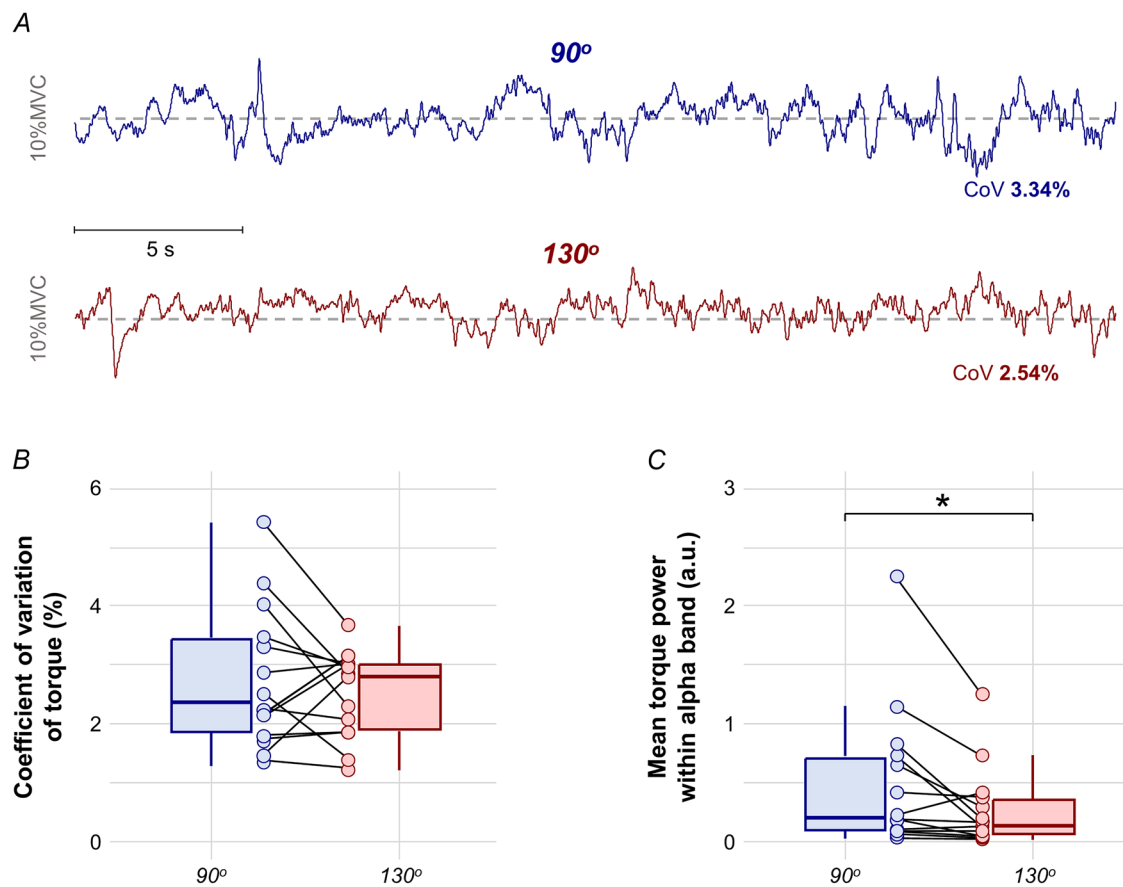


Figure 2. Force output results

A, force fluctuations for a representative participant. The blue and red lines indicate the ankle joint angle at 90° and 130° , respectively. Note that the coefficient of variation (CoV) is similar between the force signals. B, group results of CoV force. C, group results of mean force power within the alpha band. Circles identify individual participants. Horizontal traces, boxes, and whiskers denote median value, interquartile range, and distribution range. * $P < 0.05$.

the variation in dorsiflexion force output at the selected ankle joint angles (90° in blue and 130° in red) during the 10% MVC for a representative participant. The results observed for this representative participant were confirmed in the group data, showing no significant differences in force output steadiness between 90° and 130° ankle joint angles (Fig. 2B; Wilcoxon's signed-rank test; $V = 70$; $P = 0.296$). The CoV of force output values was 2.4% (1.9%–3.4%) and 2.8% (1.9%–3.0%) for 90° and 130° ankle joint angles, respectively. These results remained consistent when considering the 30 s steadiest portion within the 40 s plateau region for CoV of force calculation (90° ankle joint angle: 2.1% (1.7%–3.3%); 130° ankle joint angle: 2.4% (1.8%–2.7%); Wilcoxon's signed-rank test; $V = 70$; $P = 0.296$).

We calculated the mean force output power within the 5–15 Hz range to examine changes in force output oscillations within the alpha band between the ankle joint angles. Group results indicated a significant decrease in mean force output power values between 90° and 130° (Fig. 2C; Wilcoxon's signed-rank test; $V = 93$; $P = 0.009$). Notably, in Fig. 2C, an influential value is visible in the 90° condition (blue circle higher than 2). When excluding this participant (no. 10) from the analysis, there was still a significant decrease in mean force power between 90° and 130° (Wilcoxon's signed-rank test; $V = 79$; $P = 0.017$).

Level of common synaptic input and mean discharge rate

To evaluate changes in common synaptic input between conditions, HDsEMG signals were decomposed into their constituent motor unit spike trains. Subsequently, the average of z -coherence estimates was then quantified in the delta (0–5 Hz), alpha (5–15 Hz), and beta (15–35 Hz) bands, separately for each ankle joint angle. The same analysis was conducted considering only matched motor units between ankle joint angles. A total of 257 and 221 motor units were included for the 90° and 130° ankle joint angles, respectively, of which 132 were matched between angles. All details regarding the number of motor units included for each participant are provided in Table 1.

Two participants (no. 3 and no. 5; both males; Table 1) were excluded from the coherence analysis as only three motor units were decomposed at 130° (see Methods). Figure 3A depicts the pooled z -coherence considering all participants. As the ankle joint angle increased (increasing the TA muscle length) there was a concomitant reduction in the coherence in the 5–15 Hz bandwidth (alpha band; see highlighted yellow area in Fig. 3A). There was a significant effect of condition on the coherence values in the alpha band (Fig. 3C; LMM; $F = 24.64$; $P < 0.001$), which was not observed in either the delta (Fig. 3B; LMM; $F = 0.69$; $P = 0.422$) or the beta band (Fig. 3D; LMM;

Table 1. Number of motor units included for each participant

Participant	Ankle joint angle		Matched motor units
	90°	130°	
1	9	12	8
2	6	4	2
3	13	3	0
4	18	16	12
5	19	3	0
6	17	18	13
7	18	19	4
8	22	19	16
9	31	32	25
10	23	25	21
11	35	29	5
12	18	12	6
13	17	14	12
14	11	15	8
Total	257	221	132
Median	18	16	8
Interquartile range	14–21	12–19	4–13

$F = 2.89$; $P = 0.117$). Specifically, z -coherence values in the alpha band significantly reduced from 1.20 [0.95, 1.45] to 0.99 [0.73, 1.24] between 90° and 130° ankle joint angles. Comparable results were observed for the beta band when considering the low-beta band (15–25 Hz) and high-beta band (25–35 Hz) separately (LMM; low-beta: $F = 0.69$; $P = 0.422$; high-beta: $F = 3.71$; $P = 0.080$).

Similar results were observed when considering the matched motor units between ankle joint angles. Specifically, while coherence values in the alpha band significantly reduced between 90° and 130° (LMM; $F = 11.72$; $P = 0.007$), no significant changes were observed in either the delta (LMM; $F = 0.09$; $P = 0.767$) or the beta band (LMM; $F = 3.93$; $P = 0.076$). For this analysis, one additional male participant (no. 2; Table 1) was excluded as fewer than four motor units were matched between ankle joint angles. Furthermore, no significant changes in the mean discharge rate of matched motor units were observed between ankle joint angles (90°: 11.0 [10.01, 12.1] pulses/s; 130°: 10.8 [9.76, 11.8] pulses/s; LMM; $F = 2.05$; $P = 0.153$).

Coupling between neural drive and force output oscillations

To evaluate changes in the coupling between oscillations in neural drive and force output fluctuations, we calculated the average of z -coherence within the delta and alpha bands between the cumulative spike train of motor units and the muscle force output. There were significant increases in z -coherence values between 90° and 130°

ankle joint angles for both the delta band (from 0.29 [0.07, 0.51] to 2.22 [1.99, 2.44]; LMM; $F = 165.66$; $P < 0.001$) and the alpha band (from 0.30 [0.05, 0.55] to 1.67 [1.42, 1.93]; LMM; $F = 64.55$; $P < 0.001$).

TA twitch force

To assess how changes in muscle length affected the evoked twitches from the TA, we conducted a second set of experiments in 10 participants where electrical stimuli were applied to the common peroneal nerve. This was repeated for the ankle positioned at 90° (shortened muscle length) and 130° (lengthened muscle length). The results of a representative participant in Fig. 4A demonstrate that the duration of the TA evoked twitch increased when the ankle joint position was changed from shortened

(blue line) to lengthened (red line). This increase in twitch duration led to modifications in the low-pass filter characteristics of the TA (Fig. 4B). Specifically, both t_{peak} and $t_{50\% \text{peak}}$ values showed significant increases (Fig. 4C and D; Wilcoxon's signed-rank test; $V = 0$; $P < 0.002$ for both), while f_{co} values significantly decreased (Fig. 4E; Wilcoxon's signed-rank test; $V = 55$; $P = 0.005$) between the shortened and lengthened conditions.

Simulations results

To explore how changes in the contractile properties of motor units affect the transmission of alpha band oscillations (physiological tremor) into muscle force, we simulated two models (model 1 and model 2) of ensembles of motor neurons receiving excitatory drive

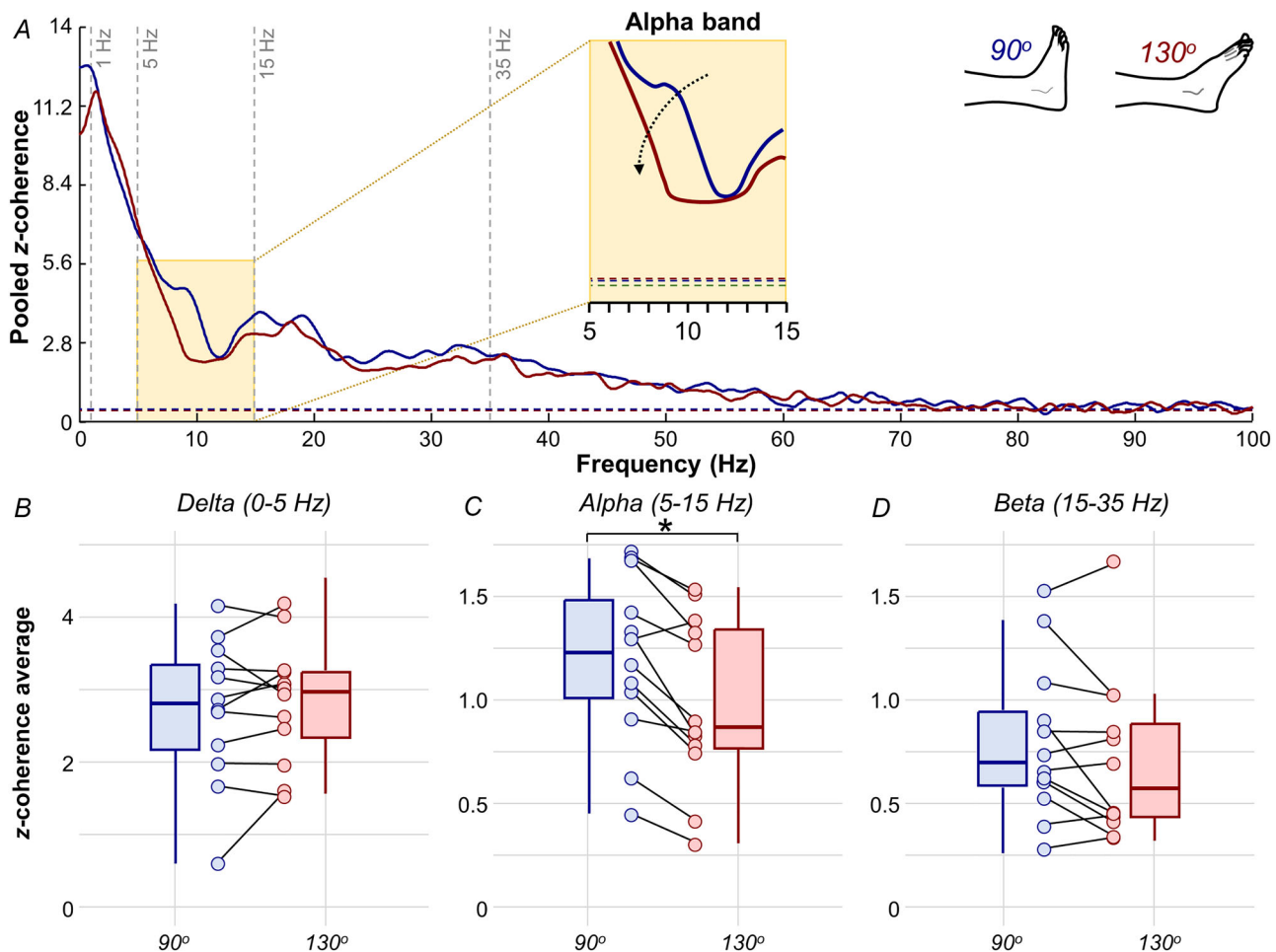


Figure 3. z-Coherence results

A, pooled z-coherence profiles considering all participants (blue for 90° and red for 130°). The horizontal dashed line indicates the confidence level. Vertical dashed lines highlight the three frequency bandwidths analysed: delta (1–5 Hz), alpha (5–15 Hz), and beta (15–35 Hz) bands. Yellow area denotes statistical differences in the z-coherence between ankle joint angles. B–D, group results of the average z-coherence for the delta (B), alpha (C), and beta (D) bands. Circles identify individual participants. Horizontal traces, boxes, and whiskers denote median value, interquartile range, and distribution range. * $P < 0.05$.

and generating isometric muscle force output. To simulate muscle lengthening conditions, we increased the twitch contraction times of individual motor units in model 2. We then calculated the z -coherence of motor units following the methodology described in the experimental data. Fig. 5A illustrates the relationship between motor unit contraction time and motor unit twitch force output for the two generated models. Visually, we observe that model 2 (red) exhibits a rightward shift towards greater twitch contraction times compared to model 1 (blue). This difference, similar to that observed in the evoked twitch results, was confirmed statistically (Fig. 5B; Wilcoxon's signed-rank test; $V = 0$; $P < 0.001$). Figure 5C shows the pooled z -coherence for the 10 realizations of each model and demonstrates a significant decrease in the z -coherence within the alpha band in model 2 compared to model 1 (Fig. 5D; LMM; $F = 16.84$; $P < 0.003$). We also observed greater z -coherence values in the delta band in model 2 compared to model 1 (LMM; $F = 95.71$; $P < 0.001$), but no

statistically significant differences were found in the beta band (LMM; $F = 2.31$; $P = 0.163$).

Discussion

The present study investigates acute adjustments in neuro-muscular control strategies based on changes in joint angle and, consequently, musculotendinous length. Our main findings revealed that changing the agonist muscle (TA) length from shorter to longer and the antagonist muscle (triceps surae) from longer to shorter induced reductions in the magnitude of agonist (TA) alpha band oscillations in the common synaptic inputs. Additionally, we explored the relation between these changes in physiological tremor and the low-pass filtering characteristics of the muscle. Our experimental results, supported by a simplified computational simulation, suggested that the increase of motor unit twitch duration resulting from increased muscle length directly influences the amplitude

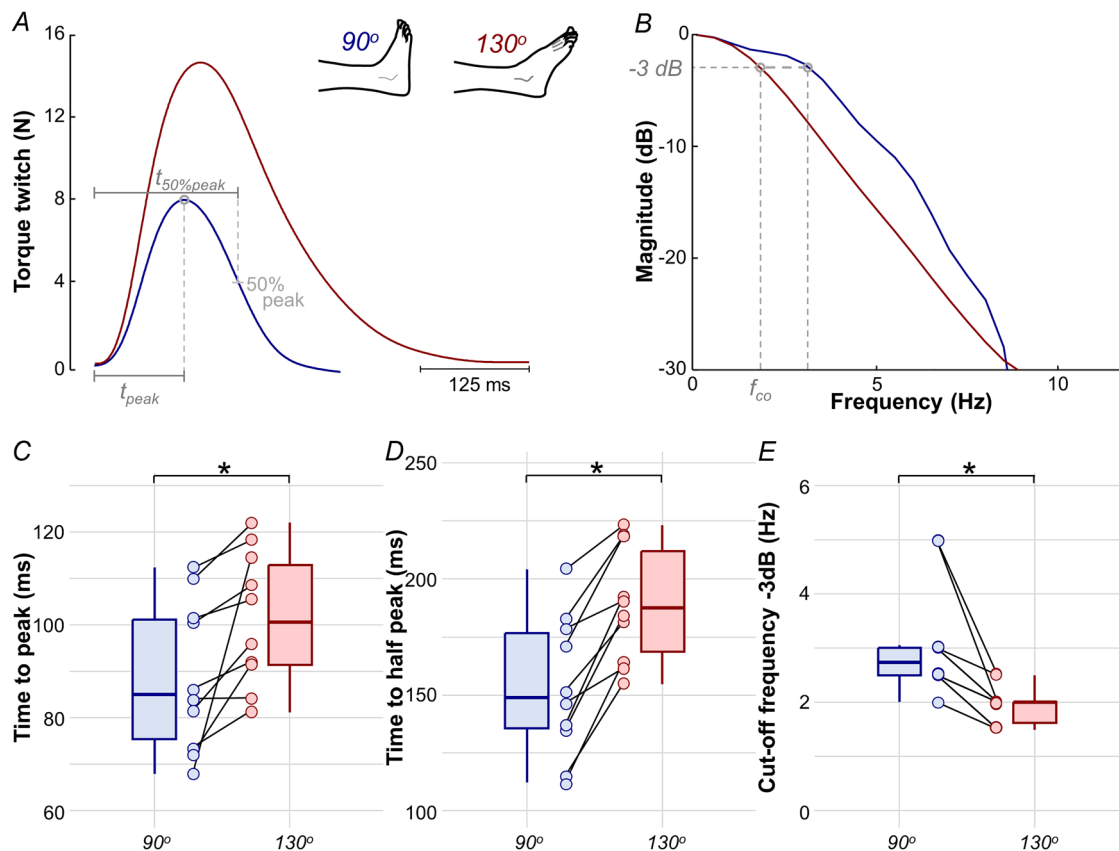


Figure 4. Twitch force results

A, twitch force signals evoked from the tibialis anterior muscle of a representative participant when electrical stimuli were applied to the common peroneal nerve. B, magnitude of the frequency response of the twitch force signals showed in A. The cut-off frequency f_{co} in which the gain was attenuated by -3 dB is indicated with the dashed grey lines. C–E, group results of the time to peak (C), time to half peak (D), and cut-off frequency f_{co} (E). Circles identify individual participants. Horizontal traces, boxes, and whiskers denote median value, interquartile range, and distribution range. * $P < 0.05$. In all panels, blue and red indicate the ankle positioned at 90° (shortened muscle length) and 130° (lengthened muscle length), respectively. t_{peak} , time to peak; $t_{50\%peak}$, time to half-peak.

of the alpha band (physiological tremor) oscillations, which may be through the proprioceptive (Ia) afferent loop.

Modulation of alpha band oscillations in motor neuron inputs with changes in muscle length

During sustained isometric contractions, shared synaptic projections to the motor neuron pool generate significant coherence between motor unit spike trains across delta, alpha, beta and even higher frequency bands. For instance, Castronovo, Negro et al. (2015) have shown significant coherence up to ~ 80 Hz during sustained isometric contractions, and these results have been consistently corroborated in subsequent studies using motor unit recordings (Muceli et al., 2022) and EMG measurements (Kerkman et al., 2018). However, due to the muscle's contractile properties, which act as a low-pass filter on

neural drive at ~ 12 Hz (Baldissera et al., 1998; Bawa & Stein, 1976), only the coherent oscillations in the delta and alpha bands are transmitted to the force signal. Therefore, these oscillations are effectively responsible for force variability (Hug et al., 2023). Considering that delta band oscillations represent the precise command for optimal force generation (De Luca et al., 1982; Farina et al., 2014; Negro et al., 2009), alpha band oscillations can be viewed as involuntary common noise inputs that limit the accuracy of the force output (i.e. force steadiness). Consequently, modulations in alpha band coherence offer an interesting mechanism to modulate neural connectivity and enhance the precision of the force output. These modulations in alpha band have primarily been attributed to the resonant behaviour of Ia afferent pathways (Cresswell & Löscher, 2000; Halliday & Redfeard, 1956; Lippold, 1970; Lippold, 1971). Moreover, previous observations in macaque monkeys

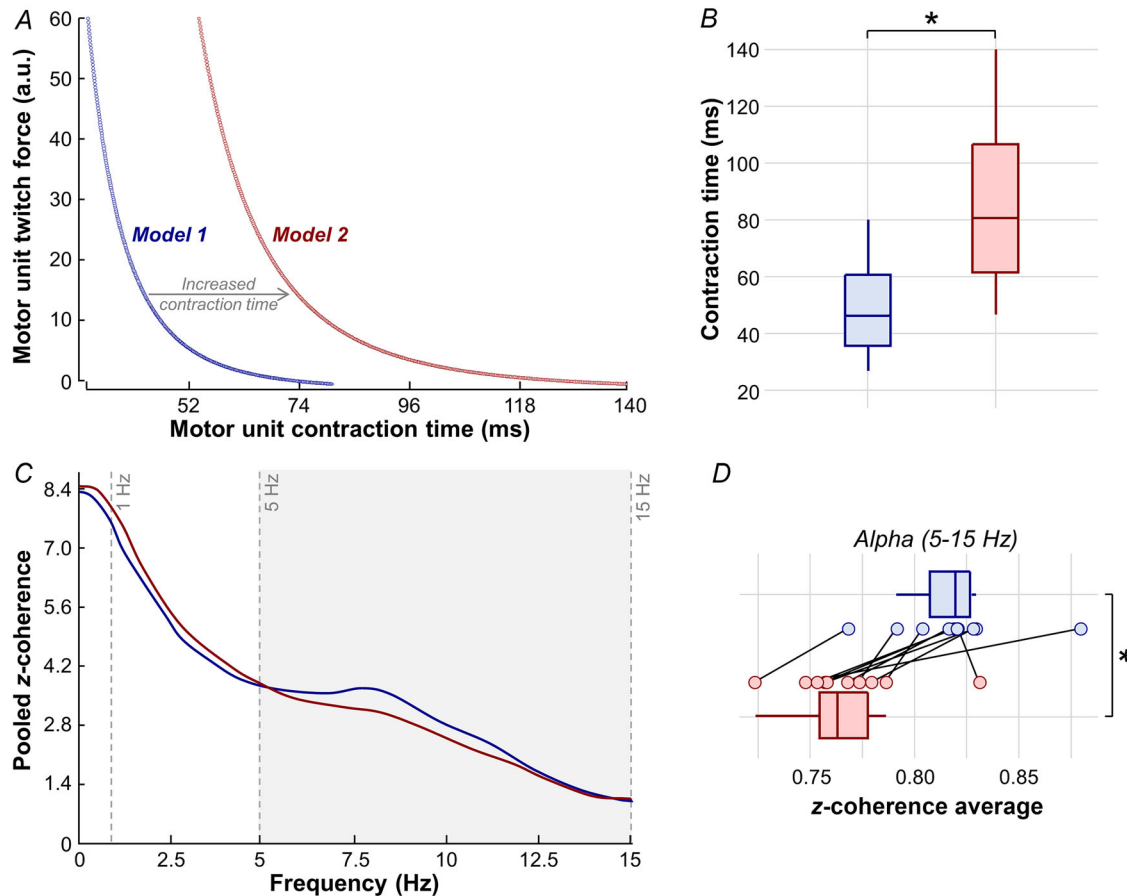


Figure 5. Simulation results

A, the relation between motor unit contraction time and motor unit twitch force output for the two generated models of ensembles of motor neurons. Note that the increase in twitch contraction times of individual motor units in model 2 (red) compared with model 1 (blue). B, comparison between motor unit contraction time of the two models. C, pooled z-coherence profiles for the 10 realizations of each model (blue for model 1 and red for model 2). D, results of z-coherence values in the alpha band for the 10 realizations of each model. Circles identify individual participants. Horizontal traces, boxes, and whiskers denote the median value, interquartile range, and distribution range. $*P < 0.05$.

have suggested that specific spinal interneurons may cancel the alpha band frequency range from cortex to motor neuron inputs, thereby reducing tremor and improving movement precision (Koželj & Baker, 2014; Williams et al., 2010). Therefore, various factors, such as the visual demand of the task (Laine et al., 2014) or pain (Yavuz et al., 2015), can modulated the tremor frequency range in the common synaptic input to motor neurons, directly influencing optimal force output control.

Consistent with these studies, our results demonstrated that manipulating muscle length provides another approach to modulate physiological tremor in the shared synaptic inputs to the alpha motor neuron pool. Specifically, by increasing the TA muscle length, we observed significant reductions in the coherence between motor unit spike trains within the alpha band, while not significantly affecting the delta or beta bands (Fig. 3B–D). These findings suggest that changing the muscle length from shorter to longer induces a reduction in the common synaptic noise input into motor neurons. Importantly, these reductions were reflected in the oscillations of muscle force output within the alpha band and an increased coupling between neural drive and muscle force output oscillations within the delta and alpha bands. This result indicates that increased muscle length offers a means to enhance the representation of shared synaptic input oscillations relevant to force control in force output.

Mechanisms involved in reducing tremor oscillations in the lengthened muscle

It has been reported that force output fluctuations due to changes in muscle length may stem from variations in the viscoelastic properties of the joint such as musculoskeletal stiffness and joint laxity or spindle Ia afferent gains and modulation in the motor unit discharge rate (Clamann & Schelhorn, 1988; Inglis & Gabriel, 2021; Jalaeddini et al., 2017; Powers & Binder, 1991; Rack & Westbury, 1969). Previous research has reported that higher stimulation frequencies are needed to achieve similar force outputs at shorter muscle lengths (Mela et al., 2001), implying the need for adjustments in motor unit discharge rates (Marsh et al., 1981; Rack & Westbury, 1969). However, when considering the same motor units between different ankle joint positions (90° and 130°), our results indicated no significant differences in mean discharge rate. These findings are consistent with previous studies demonstrating that during voluntary contractions, particularly for the TA, motor unit discharge rates remain stable across different muscle lengths (Bigland-Ritchie et al., 1992; Cudicio et al., 2022). This stability in motor unit discharge rate suggests that the effort to generate force in terms of neural drive is comparable between conditions. Therefore, it is likely that other mechanisms

contribute to the alterations in force tremor as a result of changes in muscle length (Bigland-Ritchie et al., 1992). Considering the interplay between the Ia afferent loop and physiological tremor modulations (Christakos et al., 2006; Cresswell & Löscher, 2000; Hagbarth & Young, 1979; Laine et al., 2016; Lippold, 1970), Jalaeddini et al. (2017) employed a closed-loop model to investigate whether adjustments in Ia afferent pathway gain could explain changes in force tremor at various lengths of the plantar flexors. Jalaeddini et al. (2017) reported that increased tremor with muscle shortening could be attributed to adjustments of Ia afferent gains, particularly through gamma static fusimotor drive. To further explore these findings, our study investigated another potential mechanism that could explain the reductions in tremor, both in the shared synaptic input to motor neurons and in force output, with muscle lengthening: the low pass filtering effect of the muscle. Consistent with previous findings (Bawa & Stein, 1976; Bigland-Ritchie et al., 1992; Mannard & Stein, 1973), we demonstrated that the twitch time to peak force and the time to half the peak force were significantly greater in the lengthened compared to the shortened condition (Fig. 4). These results align with expected outcomes, as the decreased joint angle results in increased pre-contraction muscle tendon unit tension in the flexed (90°) condition which facilitates a faster achievement of peak twitch force compared to the extended (130°) ankle joint position. This increased twitch duration with muscle lengthening enhances the low-pass filter characteristics of the TA (i.e. significant reduction of f_{co} with muscle lengthening, Fig. 4E), leading to alterations in the filtering of the neural drive to the muscle and, subsequently, in the Ia afferent feedback loop. Therefore, our results suggest that, in addition to fusimotor control (Jalaeddini et al., 2017), alterations in the peripheral contractile properties of motor units due to changes in muscle length have a significant impact on the transmission of the shared synaptic noise into muscle force output. These experimental findings were further supported by the simulation results, demonstrating that similar excitatory drives arriving at motor neuron ensembles with different twitch durations resulted in distinct alpha band coherence between motor unit spike trains (Fig. 5). Although, the focus of this paper was on the changes in muscle length as a result of changing the ankle joint angle, it must also be addressed that the changes in muscle length may also result in changes in muscle spindle activity. Although it was not measured in this study, the changes in muscle spindle length as a result of slack or tension in the muscle could also lead to alterations in motoneuron excitability and affect both motor unit discharge rate and force output steadiness (De Luca et al., 2009; Inglis & Gabriel, 2021). However, we did not observe any difference in motor unit discharge rate between the two ankle joint angles and subsequent

changes in muscle length. This lack of difference may suggest negligible muscle spindle influence at these two angles during low level force outputs.

Another potential mechanism that could explain our findings relates to the lengthening of the antagonist triceps surae muscle when the TA is in a shortened position at an ankle joint angle of 90°. This lengthening of the antagonist muscle may lead to a reciprocal inhibition of the dorsiflexors during contractions as both a biomechanical and neural protection mechanism to avoid injury. While not specifically addressed in this study, it is well known that reciprocal inhibition can also influence the common synaptic input oscillations to motor neurons (Yavuz et al., 2018), potentially resulting in alterations in physiological tremor in the alpha band. Although antagonist co-activation was not measured in the present study, securing the ankle joint in a position and performing isometric contractions would minimize the effect of reciprocal inhibition as it is markedly lower during isometric contractions compared to dynamic contractions (Pääsuke et al., 2001). Moreover, it is plausible that other neural pathways (both excitatory and inhibitory), such as inputs from the muscle spindles, Golgi tendon organs, joint receptors and other somatic receptors, could contribute to this phenomenon.

In the current study, there were no significant differences in force steadiness among different ankle joint positions, which aligns with previous findings in the TA muscle (Tsatsaki et al., 2022). A potential explanation for this lack of changes in force steadiness is that the CoV of force provides a global measure of the variance in the control signal received by motor neurons (Enoka & Farina, 2021) and, consequently, it may not distinguish the contributions of components related to voluntary corrections and involuntary fluctuations. Additionally, the viscoelastic properties of the muscle tendon unit acting about the ankle joint may explain why there were no changes in force steadiness at 130° compared to 90°. At a shortened tendon length (90°), there is a significant amount of slack in the musculotendinous viscoelastic properties. Consequently, the force output from the contractile tissue must overcome this slack to generate smooth movement about a joint, which may require motor unit behavioural changes such as synchronization, doublet discharges (Enoka et al., 2003; Yao et al., 2000), or the recruitment of additional motor units (Farina & Negro, 2015). Unfortunately, this may come at the expense of force output stability (Inglis & Gabriel, 2021). Conversely, placing the joint at 130° significantly reduces the slack in the system, optimizing the speed of tension transmission down the tendon's line of action, resulting in a shorter electro-mechanical delay (Yavuz et al., 2010). However, this comes at the cost of stability in force output steadiness, as the lengthened position likely increases the number of active cross-bridges and internal force (Ng

et al., 1994; Wu et al., 2019), leading to a mechanical disadvantage for steady force production. Finally, our results revealed a slight but significant increase in peak force when the ankle was secured at a joint angle of 90° compared to 130° position (~8.7%). This increase could be attributed, at least in part, to sarcomere overlengthening beyond the optimal overlap (Bigland-Ritchie et al., 1992; Petrovic et al., 2022).

Limitations

The positioning of participants during testing is a potential limitation of the study that may have influenced the results. In this study, subjects were seated with the test leg extended. Mitchell et al. (2008) reported that the range of motion of the ankle joint can be significantly inhibited based on the position of the pelvis and hip and knee joints. Their study demonstrated that when the knee is flexed (90°) compared to extended (180°) in a seated position, the ankle joint's passive range of motion changes from 47.3° to 16.4°, representing almost a 65% reduction in the range of motion. Changes in the hip and knee angles may either increase or decrease tension in the passive tissues. Therefore, straightening the leg while seated may passively increase tension in the nerves, muscles, and tendons from the lumbar spine to the foot, potentially influencing the range of motion of the ankle joint. However, the evident changes in peak force among ankle joint angles suggest that we successfully investigated positions at both shortened and lengthened relative to an optimal length. Additionally, flexing the knee would naturally induce a shortening in the biarticular triceps surae muscle, which could be a potential confounding factor.

Conclusions

Our study explored the relationship between muscle length changes and neural changes affecting isometric dorsiflexion force production. We observed that changing the TA muscle length from shorter to longer (and the triceps surae muscle length from longer to shorter) resulted in decreases in alpha band oscillations (physiological tremor) both in the shared synaptic input to motor neurons and in force output. Importantly, our findings suggest that alterations in the average motor unit twitch duration contribute to these observed effects, influencing the synaptic input to the motor neuron pools through the Ia afferent loop and, consequently, the neural drive to motor neurons. Therefore, the current study provides valuable insights into the interplay between muscle biomechanics and neural adjustments, while illuminating potential neuromechanical mechanisms underlying force production and control. These results may be utilized

in either clinical populations or the elderly in the prescription of rehabilitation strategies to focus more on proprioceptive feedback during recovery (i.e. post-stroke, post-fall).

References

- Baker, S. N., Olivier, E., & Lemon, R. N. (1997). Coherent oscillations in monkey motor cortex and hand muscle EMG show task-dependent modulation. *The Journal of Physiology*, **501**(Pt 1), 225–241.
- Baker, S. N., Pinches, E. M., & Lemon, R. N. (2003). Synchronization in monkey motor cortex during a precision grip task. II. effect of oscillatory activity on corticospinal output. *Journal of Neurophysiology*, **89**(4), 1941–1953.
- Baldissera, F., Cavallari, P., & Cerri, G. (1998). Motoneuronal pre-compensation for the low-pass filter characteristics of muscle. A quantitative appraisal in cat muscle units. *The Journal of Physiology*, **511**(Pt 2), 611–627.
- Bawa, P., & Stein, R. B. (1976). Frequency response of human soleus muscle. *Journal of Neurophysiology*, **39**(4), 788–793.
- Berniker, M., Jarc, A., Bizzi, E., & Tresch, M. C. (2009). Simplified and effective motor control based on muscle synergies to exploit musculoskeletal dynamics. *Proceedings of the National Academy of Sciences, USA*, **106**(18), 7601–7606.
- Bigland-Ritchie, B. R., Furbush, F. H., Gandevia, S. C., & Thomas, C. K. (1992). Voluntary discharge frequencies of human motoneurons at different muscle lengths. *Muscle & Nerve*, **15**(2), 130–137.
- Bräcklein, M., Barsakcioglu, D. Y., Del Vecchio, A., Ibáñez, J., & Farina, D. (2022). Reading and modulating cortical β bursts from motor unit spiking activity. *The Journal of Neuroscience*, **42**(17), 3611–3621.
- Bremner, F. D., Baker, J. R., & Stephens, J. A. (1991). Correlation between the discharges of motor units recorded from the same and from different finger muscles in man. *The Journal of Physiology*, **432**(1), 355–380.
- Castronovo, A. M., Negro, F., Conforto, S., & Farina, D. (2015). The proportion of common synaptic input to motor neurons increases with an increase in net excitatory input. *Journal of Applied Physiology*, **119**(11), 1337–1346.
- Castronovo, A. M., Negro, F., & Farina, D. (2015). Theoretical model and experimental validation of the estimated proportions of common and independent input to motor neurons. *Annual International Conference of the IEEE Engineering in Medicine and Biology Society*, **2015**, 254–257.
- Christakos, C. N., Papadimitriou, N. A., & Erimaki, S. (2006). Parallel neuronal mechanisms underlying physiological force tremor in steady muscle contractions of humans. *Journal of Neurophysiology*, **95**(1), 53–66.
- Clamann, H. P., & Schelhorn, T. B. (1988). Nonlinear force addition of newly recruited motor units in the cat hindlimb. *Muscle & Nerve*, **11**, 1079–1089.
- Cogliati, M., Cudicio, A., Martinez-Valdes, E., Tarperi, C., Schena, F., Orizio, C., & Negro, F. (2020). Half marathon induces changes in central control and peripheral properties of individual motor units in master athletes. *Journal of Electromyography and Kinesiology*, **55**, 102472.
- Conway, B. A., Halliday, D. M., Farmer, S. F., Shahani, U., Maas, P., Weir, A. I., & Rosenberg, J. R. (1995). Synchronization between motor cortex and spinal motoneuronal pool during the performance of a maintained motor task in man. *The Journal of Physiology*, **489**(Pt 3), 917–924.
- Cresswell, A. G., & Löscher, W. N. (2000). Significance of peripheral afferent input to the alpha-motoneurone pool for enhancement of tremor during an isometric fatiguing contraction. *European Journal of Applied Physiology*, **82**(1–2), 129–136.
- Cudicio, A., Martinez-Valdes, E., Cogliati, M., Orizio, C., & Negro, F. (2022). The force-generation capacity of the tibialis anterior muscle at different muscle-tendon lengths depends on its motor unit contractile properties. *European Journal of Applied Physiology*, **122**(2), 317–330.
- D'Avella, A., & Bizzi, E. (2005). Shared and specific muscle synergies in natural motor behaviors. *Proceedings of the National Academy of Sciences, USA*, **102**(8), 3076–3081.
- Datta, A. K., Farmer, S. F., & Stephens, J. A. (1991). Central nervous pathways underlying synchronization of human motor unit firing studied during voluntary contractions. *The Journal of Physiology*, **432**(1), 401–425.
- Datta, A. K., & Stephens, J. A. (1990). Synchronization of motor unit activity during voluntary contraction in man. *The Journal of Physiology*, **422**(1), 397–419.
- De Luca, C. J., Gonzalez-Cueto, J. A., Bonato, P., & Adam, A. (2009). Motor unit recruitment and proprioceptive feedback decrease the common drive. *Journal of Neurophysiology*, **101**(3), 1620–1628.
- De Luca, C. J., Lefever, R. S., Mccue, M. P., & Xenakis, A. P. (1982). Control scheme governing concurrently active human motor units during voluntary contractions. *The Journal of Physiology*, **329**(1), 129–142.
- Dideriksen, J., Elias, L. A., Zambalde, E. P., Germer, C. M., Molinari, R. G., & Negro, F. (2022). Influence of central and peripheral motor unit properties on isometric muscle force entropy: A computer simulation study. *Journal of Biomechanics*, **139**, 110866.
- Dideriksen, J. L., & Negro, F. (2018). Spike-triggered averaging provides inaccurate estimates of motor unit twitch properties under optimal conditions. *Journal of Electromyography and Kinesiology*, **43**, 104–110.
- Dideriksen, J. L., Negro, F., Enoka, R. M., & Farina, D. (2012). Motor unit recruitment strategies and muscle properties determine the influence of synaptic noise on force steadiness. *Journal of Neurophysiology*, **107**(12), 3357–3369.
- Duchateau, J., & Enoka, R. M. (2011). Human motor unit recordings: Origins and insight into the integrated motor system. *Brain Research*, **1409**, 42–61.
- Enoka, R. M., Christou, E. A., Hunter, S. K., Kornatz, K. W., Semmler, J. G., Taylor, A. M., & Tracy, B. L. (2003). Mechanisms that contribute to differences in motor performance between young and old adults. *Journal of Electromyography and Kinesiology*, **13**(1), 1–12.
- Enoka, R. M., & Farina, D. (2021). Force steadiness: From motor units to voluntary actions. *Physiology (Bethesda, Md.)*, **36**, 114–130.

- Farina, D., & Negro, F. (2015). Common synaptic input to motor neurons, motor unit synchronization, and force control. *Exercise and Sport Sciences Reviews*, **43**(1), 23–33.
- Farina, D., Negro, F., & Dideriksen, J. L. (2014). The effective neural drive to muscles is the common synaptic input to motor neurons. *The Journal of Physiology*, **592**(16), 3427–3441.
- Farmer, S. F., Bremner, F. D., Halliday, D. M., Rosenberg, J. R., & Stephens, J. A. (1993). The frequency content of common synaptic inputs to motoneurons studied during voluntary isometric contraction in man. *The Journal of Physiology*, **470**(1), 127–155.
- Feeney, D. F., Mani, D., & Enoka, R. M. (2018). Variability in common synaptic input to motor neurons modulates both force steadiness and pegboard time in young and older adults. *The Journal of Physiology*, **596**(16), 3793–3806.
- Feinstein, B., Lindegård, B., Nyman, E., & Wohlfart, G. (1955). Morphologic studies of motor units in normal human muscles. *Acta Anatomica*, **23**(2), 127–142.
- Fuglevand, A. J., Winter, D. A., & Patla, A. E. (1993). Models of recruitment and rate coding organization in motor-unit pools. *Journal of Neurophysiology*, **70**(6), 2470–2488.
- Gallet, C., & Julien, C. (2011). The significance threshold for coherence when using the Welch's periodogram method: Effect of overlapping segments. *Biomedical Signal Processing and Control*, **6**(4), 405–409.
- Gogeaşcochea, A., Ornelas-Kobayashi, R., Yavuz, U. S., & Sartori, M. (2023). Characterization of motor unit firing and twitch properties for decoding musculoskeletal force in the human ankle joint in vivo. *IEEE Transactions on Neural Systems and Rehabilitation Engineering*, **31**, 4040–4050.
- Hagbarth, K.-E., & Young, R. R. (1979). Participation of the stretch reflex in human physiological tremor. *Brain*, **102**(3), 509–526.
- Halliday, A. M., & Redfearn, J. W. T. (1956). An analysis of the frequencies of finger tremor in healthy subjects. *The Journal of Physiology*, **134**(3), 600–611.
- Hassan, A., Thompson, C. K., Negro, F., Cummings, M., Powers, R. K., Heckman, C. J., Dewald, J. P. A., & McPherson, L. M. (2020). Impact of parameter selection on estimates of motoneuron excitability using paired motor unit analysis. *Journal of Neural Engineering*, **17**(1), 016063.
- Heckman, C. J., & Enoka, R. M. (2012). Motor unit. *Comprehensive Physiology*, **2**, 2629–2682.
- Henderson, T. T., Thorstensen, J. R., Morrison, S., Tucker, M. G., & Kavanagh, J. J. (2022). Physiological tremor is suppressed and force steadiness is enhanced with increased availability of serotonin regardless of muscle fatigue. *Journal of Neurophysiology*, **127**(1), 27–37.
- Hug, F., Avrillon, S., Del Vecchio, A., Casolo, A., Ibanez, J., Nuccio, S., Rossato, J., Holobar, A., & Farina, D. (2021). Analysis of motor unit spike trains estimated from high-density surface electromyography is highly reliable across operators. *Journal of Electromyography and Kinesiology*, **58**, 102548.
- Hug, F., Avrillon, S., Ibáñez, J., & Farina, D. (2023). Common synaptic input, synergies and size principle: Control of spinal motor neurons for movement generation. *The Journal of Physiology*, **601**(1), 11–20.
- Inglis, J. G., & Gabriel, D. A. (2021). Sex differences in the modulation of the motor unit discharge rate leads to reduced force steadiness. *Applied Physiology, Nutrition and Metabolism*, **46**(9), 1065–1072.
- Ishizuka, N., Mannen, H., Hongo, T., & Sasaki, S. (1979). Trajectory of group Ia afferent fibers stained with horseradish peroxidase in the lumbosacral spinal cord of the cat: Three dimensional reconstructions from serial sections. *Journal of Comparative Neurology*, **186**(2), 189–211.
- Jalaleddini, K., Nagamori, A., Laine, C. M., Golkar, M. A., Kearney, R. E., & Valero-Cuevas, F. J. (2017). Physiological tremor increases when skeletal muscle is shortened: Implications for fusimotor control. *The Journal of Physiology*, **595**(24), 7331–7346.
- Kaneda, K., Wakabayashi, H., Sato, D., Uekusa, T., & Nomura, T. (2008). Lower extremity muscle activity during deep-water running on self-determined pace. *Journal of Electromyography and Kinesiology*, **18**(6), 965–972.
- Kerkman, J. N., Daffertshofer, A., Gollo, L. L., Breakspear, M., & Boonstra, T. W. (2018). Network structure of the human musculoskeletal system shapes neural interactions on multiple time scales. *Science Advances*, **4**(6), eaat0497.
- Kirkwood, P. A., & Sears, T. A. (1978). The synaptic connexions to intercostal motoneurons as revealed by the average common excitation potential. *The Journal of Physiology*, **275**(1), 103–134.
- Koželj, S., & Baker, S. N. (2014). Different phase delays of peripheral input to primate motor cortex and spinal cord promote cancellation at physiological tremor frequencies. *Journal of Neurophysiology*, **111**(10), 2001–2016.
- Kuznetsova, A., Brockhoff, P. B., & Christensen, R. H. B. (2017). lmerTest package: Tests in linear mixed effects models. *Journal of Statistical Software*, **82**(13), 1–26.
- Laine, C. M., Martinez-Valdes, E., Falla, D., Mayer, F., & Farina, D. (2015). Motor neuron pools of synergistic thigh muscles share most of their synaptic input. *The Journal of Neuroscience*, **35**(35), 12207–12216.
- Laine, C. M., Nagamori, A., & Valero-Cuevas, F. J. (2016). The dynamics of voluntary force production in afferented muscle influence involuntary tremor. *Frontiers in Computational Neuroscience*, **10**, 86.
- Laine, C. M., Yavuz, Ş. U., & Farina, D. (2014). Task-related changes in sensorimotor integration influence the common synaptic input to motor neurons. *Acta Physiologica*, **211**(1), 229–239.
- Lemon, R. N. (2008). Descending pathways in motor control. *Annual Review of Neuroscience*, **31**(1), 195–218.
- Lenth, R., Singmann, H., Love, J., Buerkner, P., & Herve, M. (2019). Package 'emmeans'.
- Lippold, O. (1971). Physiological tremor. *Scientific American*, **224**(3), 65–73.
- Lippold, O. C. J. (1970). Oscillation in the stretch reflex arc and the origin of the rhythmical, 8–12 C-S component of physiological tremor. *The Journal of Physiology*, **206**(2), 359–382.
- Mannard, A., & Stein, R. B. (1973). Determination of the frequency response of isometric soleus muscle in the cat using random nerve stimulation. *The Journal of Physiology*, **229**(2), 275–296.

- Marsh, E., Sale, D., Mccomas, A. J., & Quinlan, J. (1981). Influence of joint position on ankle dorsiflexion in humans. *Journal of Applied Physiology*, **51**(1), 160–167.
- Martinez-Valdes, E., Negro, F., Laine, C. M., Falla, D., Mayer, F., & Farina, D. (2017). Tracking motor units longitudinally across experimental sessions with high-density surface electromyography. *The Journal of Physiology*, **595**(5), 1479–1496.
- Mcauley, J. H. (2000). Physiological and pathological tremors and rhythmic central motor control. *Brain*, **123**(Pt 8), 1545–1567.
- Mcmanus, L., Flood, M. W., & Lowery, M. M. (2019). Beta-band motor unit coherence and nonlinear surface EMG features of the first dorsal interosseous muscle vary with force. *Journal of Neurophysiology*, **122**(3), 1147–1162.
- Mela, P., Veltink, P. H., & Huijting, P. A. (2001). The influence of stimulation frequency and ankle joint angle on the moment exerted by human dorsiflexor muscles. *Journal of Electromyography and Kinesiology*, **11**(1), 53–63.
- Mitchell, B., Bressel, E., Mcnair, P. J., & Bressel, M. E. (2008). Effect of pelvic, hip, and knee position on ankle joint range of motion. *Physical Therapy in Sport*, **9**(4), 202–208.
- Muceli, S., Poppendieck, W., Holobar, A., Gandevia, S., Liebetanz, D., & Farina, D. (2022). Blind identification of the spinal cord output in humans with high-density electrode arrays implanted in muscles. *Science Advances*, **8**(46), eabo5040.
- Negro, F., & Farina, D. (2011). Linear transmission of cortical oscillations to the neural drive to muscles is mediated by common projections to populations of motoneurons in humans. *The Journal of Physiology*, **589**(3), 629–637.
- Negro, F., & Farina, D. (2012). Factors influencing the estimates of correlation between motor unit activities in humans. *PLoS ONE*, **7**(9), e44894.
- Negro, F., Holobar, A., & Farina, D. (2009). Fluctuations in isometric muscle force can be described by one linear projection of low-frequency components of motor unit discharge rates. *The Journal of Physiology*, **587**(24), 5925–5938.
- Negro, F., Muceli, S., Castronovo, A. M., Holobar, A., & Farina, D. (2016). Multi-channel intramuscular and surface EMG decomposition by convolutive blind source separation. *Journal of Neural Engineering*, **13**(2), 026027.
- Ng, A. V., Agre, J. C., Hanson, P., Harrington, M. S., & Nagle, F. J. (1994). Influence of muscle length and force on endurance and pressor responses to isometric exercise. *Journal of Applied Physiology*, **76**(6), 2561–2569.
- Nordstrom, M. A., Fuglevand, A. J., & Enoka, R. M. (1992). Estimating the strength of common input to human motoneurons from the cross-correlogram. *The Journal of Physiology*, **453**(1), 547–574.
- Pääsuke, M., Ereline, J., & Gapeyeva, H. (2001). Knee extension strength and vertical jumping performance in nordic combined athletes. *Journal of Sports Medicine and Physical Fitness*, **41**, 354–361.
- Petrovic, I., Amiridis, I. G., Holobar, A., Trypidakis, G., Kellis, E., & Enoka, R. M. (2022). Leg dominance does not influence maximal force, force steadiness, or motor unit discharge characteristics. *Medicine & Science in Sports & Exercise*, **54**.
- Powers, R. K., & Binder, M. D. (1991). Effects of low-frequency stimulation on the tension-frequency relations of fast-twitch motor units in the cat. *Journal of Neurophysiology*, **66**(3), 905–918.
- Rack, P. M. H., & Westbury, D. R. (1969). The effects of length and stimulus rate on tension in the isometric cat soleus muscle. *The Journal of Physiology*, **204**(2), 443–460.
- Rossato, J., Tucker, K., Avrillon, S., Lacourpaille, L., Holobar, A., & Hug, F. (2022). Less common synaptic input between muscles from the same group allows for more flexible coordination strategies during a fatiguing task. *Journal of Neurophysiology*, **127**(2), 421–433.
- Sears, T. A., & Stagg, D. (1976). Short-term synchronization of intercostal motoneurone activity. *The Journal of Physiology*, **263**(3), 357–381.
- Taylor, A. M., Steege, J. W., & Enoka, R. M. (2002). Motor-unit synchronization alters spike-triggered average force in simulated contractions. *Journal of Neurophysiology*, **88**(1), 265–276.
- Thompson, C. K., Negro, F., Johnson, M. D., Holmes, M. R., Mcpherson, L. M., Powers, R. K., Farina, D., & Heckman, C. J. (2018). Robust and accurate decoding of motoneuron behaviour and prediction of the resulting force output. *The Journal of Physiology*, **596**(14), 2643–2659.
- Tsatsaki, E., Amiridis, I. G., Holobar, A., Trypidakis, G., Arabatzi, F., Kellis, E., & Enoka, R. M. (2022). The length of tibialis anterior does not influence force steadiness during submaximal isometric contractions with the dorsiflexors. *European Journal of Sport Science*, **22**(4), 539–548.
- Williams, E. R., Soteropoulos, D. S., & Baker, S. N. (2010). Spinal interneuron circuits reduce approximately 10-Hz movement discontinuities by phase cancellation. *Proceedings of the National Academy of Sciences*, **107**(24), 11098–11103.
- Wu, R., Delahunt, E., Ditroilo, M., Lowery, M. M., Segurado, R., & De Vito, G. (2019). Changes in knee joint angle affect torque steadiness differently in young and older individuals. *Journal of Electromyography and Kinesiology*, **47**, 49–56.
- Yao, W., Fuglevand, R. J., & Enoka, R. M. (2000). Motor-unit synchronization increases EMG amplitude and decreases force steadiness of simulated contractions. *Journal of Neurophysiology*, **83**(1), 441–452.
- Yavuz, Ş. U., Şendemir-Ürkmez, A., & Türker, K. S. (2010). Effect of gender, age, fatigue and contraction level on electromechanical delay. *Clinical Neurophysiology*, **121**(10), 1700–1706.
- Yavuz, U. Ş., Negro, F., Diedrichs, R., & Farina, D. (2018). Reciprocal inhibition between motor neurons of the tibialis anterior and triceps surae in humans. *Journal of Neurophysiology*, **119**(5), 1699–1706.
- Yavuz, U. Ş., Negro, F., Falla, D., & Farina, D. (2015). Experimental muscle pain increases variability of neural drive to muscle and decreases motor unit coherence in tremor frequency band. *Journal of Neurophysiology*, **114**(2), 1041–1047.

Additional information

Data availability statement

All individual data of motor unit discharge times recorded at 90° and 130° are available at <https://doi.org/10.6084/m9.figshare.24631191>

Competing interests

The authors declare no competing financial interests.

Author contributions

C.O., U.S.Y. and F.N. contributed to study design; A.C. and M.C. acquired the data; H.V.C. and F.N. analysed the data; H.V.C., J.G.I. and F.N. interpreted the data; H.V.C., J.G.I. and F.N. drafted the manuscript; H.V.C., J.G.I., A.C., M.C., C.O., U.S.Y. and F.N. revised and edited the manuscript. All authors have approved the final version of the manuscript and agree to be accountable for all aspects of the work ensuring that questions related to the accuracy or integrity of any part of the work are appropriately

investigated and resolved. All persons designated as authors qualify for authorship, and all those who qualify for authorship are listed.

Funding

This study was funded by the European Research Council Consolidator Grant INCEPTION (contract no. 101045605).

Keywords

common synaptic input, force control, motor unit, muscle mechanics, twitch force

Supporting information

Additional supporting information can be found online in the Supporting Information section at the end of the HTML view of the article. Supporting information files available:

Peer Review History